BIOCHEMISTRY
including biophysical chemistry & molecular biology

Article

pubs.acs.org/biochemistry

Loop Electrostatics Asymmetry Modulates the Preexisting Conformational Equilibrium in Thrombin

Nicola Pozzi,[*,†] Mirco Zerbetto,[§] Laura Acquasaliente,[‡] Simone Tescari,[‡] Diego Frezzato,[§] Antonino Polimeno,[§] David W. Gohara,[†] Enrico Di Cera,[*,†] and Vincenzo De Filippis[*,‡]

[†]Edward A. Doisy Department of Biochemistry and Molecular Biology, Saint Louis University School of Medicine, St. Louis, Missouri 63104, United States

[‡]Department of Pharmaceutical Sciences and [§]Department of Chemical Sciences, University of Padua, via F. Marzolo 1, 35131 Padua, Italy

Supporting Information

ABSTRACT: Thrombin exists as an ensemble of active (E) and inactive (E*) conformations that differ in their accessibility to the active site. Here we show that redistribution of the E*−E equilibrium can be achieved by perturbing the electrostatic properties of the enzyme. Removal of the negative charge of the catalytic Asp102 or Asp189 in the primary specificity site destabilizes the E form and causes a shift in the 215−217 segment that compromises substrate entrance. Solution studies and existing structures of D102N document stabilization of the E* form. A new high-resolution structure of D189A also reveals the mutant in the collapsed E* form. These findings establish a new paradigm for the control of the E*−E equilibrium in the trypsin fold.

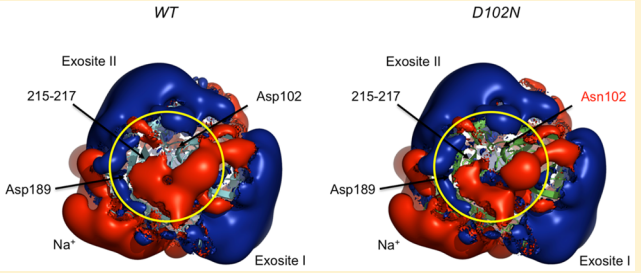

Four protease families account for more than 40% of all proteolytic enzymes in humans and are responsible for digestion, blood coagulation, fibrinolysis, development, fertilization, apoptosis, and immunity.[1,2] Trypsin-like proteases constitute the largest group and utilize a canonical catalytic triad for activity, composed of the highly conserved residues His57, Asp102, and Ser195. Catalysis is assisted by the oxyanion hole, defined by the backbone N atoms of Gly193 and Ser195, the 215−217 segment shaping the wall of the primary specificity pocket, and residue Asp189 at the bottom of this pocket that engages the Arg residue position P1 of the substrate.[3]

Thrombin is a trypsin-like protease that plays opposing functional roles in blood coagulation because of the interaction with numerous macromolecular substrates, receptors, and inhibitors.[4] Recent studies have demonstrated that thrombin exists in equilibrium between active (E) and inactive (E*) species, or ensembles.[5−8] Conformational transitions for this enzyme unfold over different time scales: a slow time scale (45 ms) for the interconversion of the E* and E ensembles detected by stopped-flow measurements[9] and a fast time scale for the interconversion of conformers within each ensemble inferred by nuclear magnetic resonance and molecular dynamics (MD) simulations.[10−13] Thrombin dynamics involve structural fluctuations of flexible loops surrounding the active site, the Na^+ binding loops, and the 215−217 segment within the active site. Movement of the 215−217 segment is a structural signature of the trypsin fold that controls access to the active site in the protease and zymogen. Binding of Na^+ shifts the preexisting E*−E equilibrium in favor of the active E form and also stabilizes more active conformers within the E ensemble, resulting in higher catalytic activity.[9] Interestingly, the allosteric effect of Na^+ on thrombin is selectively abrogated by the S195T replacement,[14] establishing a linkage between residues within the active site and conformational dynamics of the enzyme. In this context, the role of the catalytic Asp102 merits attention. One of the carboxylate oxygen atoms of Asp102 accepts hydrogen bonds from the main-chain amide groups of residues 56 and 57, and the second oxygen accepts hydrogen bonds from both the Nδ1 atom of His57 and the Oγ atom of Ser214. The negatively charged Asp102 maintains the unprotonated Nε2 with a lone pair of electrons as the general base catalyst for transfer of the proton from Oγ of Ser195 to the leaving group. Mutation of Asp to Asn does not change the number of hydrogen bonds but dramatically reverts the directionality of this network. Hence, Ser195 becomes a weak nucleophile, and the catalytic activity of the mutant D102N is compromised by 4 orders of magnitude.[15,16] Similarly, replacement of the negatively charged Asp189 with Ala and Asn in the primary specificity site compromises the specificity of thrombin toward synthetic and physiological substrates by up to 4 orders of magnitude and unexpectedly abrogates monovalent cation binding.[17] Because Asp102 and Asp189 are negatively charged at physiological pH, modifications of their

Received: April 23, 2016
Revised: May 27, 2016
Published: June 27, 2016

DOI: 10.1021/acs.biochem.6b00385
Biochemistry 2016, 55, 3984−3994

electrostatic potential could also propagate in a long-range manner within the active site and reach the flexible loops on the surface of the enzyme. Here we show that perturbation of the electrostatics within the active site and primary specificity site of thrombin has a drastic influence on the E*−E equilibrium and provide a mechanistic framework for the interpretation of key functional and structural features of the enzyme.

MATERIALS AND METHODS

Materials. α-Thrombin purified from human plasma was obtained from Haematologic Technologies (Essex Junction, VT) and buffer exchanged using an FF G-25 HiTrap column equilibrated with 5 mM Tris-HCl buffer (pH 8.0) and 0.2 M ChCl. Thrombin WT and mutants D102N and D189A were expressed in BHK cells and purified to homogeneity as described previously.[15,17,18] Peptides Hir(1−47) and Hir(48−64) were obtained by solid-phase synthesis using standard fluorenylmethyloxycarbonyl chloride (Fmoc) chemistry on a model PS3 automated synthesizer from Protein Technologies (Tucson, AZ) and purified by reverse-phase high-performance liquid chromatography.[19] Chemical identity was established by enzymatic fingerprint analysis and high-resolution mass spectrometry on a Mariner ESI-TOF instrument from Perseptive Biosystems (Stafford, TX). Nα-Fmoc-protected amino acids, solvents, and reagents for peptide synthesis were purchased from Applied Biosystems (Foster City, CA) or Bachem AG (Bubendorf, Switzerland). *p*-Aminobenzamidine (PABA), trypsin, salts, urea, and organic solvents were of analytical grade (Sigma, St. Louis, MO).

Electrostatic Calculations. The E open conformation of thrombin was obtained from the crystallographic structure of α-thrombin [Protein Data Bank (PDB) entry 1PPB] after removal of the inhibitor (PPACK), water molecules, and the coordinates of 4-(2-hydroxyethyl)-1-piperazineethanesulfonic acid (HEPES).[20] After Asp102 had been substituted with Asn, PQR files were prepared and calculations were performed using APBS[21] and BLUUES,[22] which is based on the generalized Born (GB) models.[23] Calculations were run on the nonglycosylated X-ray structure of thrombin wild type and mutant D102N, which was obtained by mutating Asp102 to Asn while keeping all other coordinates unchanged. Calculations were performed using a solvent dielectric of 78.14 and a protein dielectric of 2.0 at 298 K in 145 mM NaCl. Final electrostatic maps were constructed by subtracting the protein self-energies from the calculated map using the dxmath utility in APBS.

Molecular Dynamics Simulations. Glycosylated thrombin was solvated with 21116 explicit water molecules in a 90 Å side length cubic box. Na^+ and Cl^- ions were added, with a NaCl concentration of 0.145 M. The glycosylation was added at Asn60g according to the carbohydrate composition previously determined by Nilsson et al.[24] (Figure S1). The model was completed by creating the connectivity among the eight cysteines to generate the four disulfide bonds: Cys1−Cys122, Cys42−Cys58, Cys168−Cys182, and Cys191−Cys220. The CHARMM-27 all-atom force field with CMAP correction[25] was used for the protein and ions; the TIP3P force field was used for water molecules, whereas the carbohydrate Chain Solution Force Field (CSFF) was used for the oligosaccharide tail.[26] The pK_a of all the charged residues was calculated using the pKaTool software[27] to determine the protonation state of the amino acids in the protein at pH 7. NAMD version 2.9[28] was used to run the simulations. Briefly, after an energy minimization stage, thrombin was gradually heated by linearly changing the temperature from 1 to 310 K at a rate of 1 K/ps and then equilibrated at 310 K for 15 ns. All the simulations were run in the canonical (*NPT*) ensemble. For the wild-type protein, a 90 ns production run was performed starting from the equilibrated system. For the D102N mutant, the same parameters were used for the last 50 ns of the simulations, which was preceded by the alchemical morphing (40 ns) of residue 102 from the negative Asp to the neutral Asn. This numerical experiment was conducted to dissect the effect of charge and steric variations upon Asp to Asn mutation. The alchemical morphing was conducted in five steps. In the first four steps, the overall charge of D102 was incrementally changed from −1 to 0 (in units of electron charge in absolute value) according to the linear interpolation $q_i(\xi) = (1 - \xi)q_i^{(\mathrm{Asp})} + \xi q_i^{(\mathrm{Asn})}$. The parameter ξ assumed values of 0, 0.25, 0.5, 0.75, and 1 (Figure S2). When $\xi = 0$, the Asp residue charges are assigned to all the Asp102 atoms. When $\xi = 1$, an artificially mutated Asp102 residue is created in which the atoms have the charges of Asn (O2 of the carboxylate group of Asp102 collects the global charge of 0 of the -NH_2 moiety in Asn102). After each charge change, we let the system evolve for a total of 10 ns. After completion of the charge morphing, O2 of the carboxylate group of Asp102 was replaced with the -NH_2 moiety of Asn102; then the MD simulation of the fully mutated protein was forwarded for a further 50 ns. Thus, the total run time was identical for both WT and D102N, i.e., 90 ns, and the same simulation parameters were applied: 2 fs integration time step, all bonds with hydrogen atoms kept fixed, periodic boundary conditions, short- and long-range interactions evaluated at each MD step, nonbonded cutoff of 12 Å (with function switching at 10 Å), together with a pair list distance of 13.5 Å. The particle mesh Ewald (PME) model was used for electrostatic calculations (grid size of 90 Å in all directions of space, PME tolerance of 10^{-6}). To simulate the canonical *NPT* conditions, the system was coupled to a stochastic thermostat with a set point temperature of 310 K (with a dumping constant of 1 ps^{-1}) and to a stochastic barostat with a set point pressure of 1 atm (piston period of 100 fs, piston decay time of 50 fs). The Cα−Cα variance−covariance matrix, **M**, was used to map the conformational flexibility profile resulting from Asp102 to Asn mutation. The matrix elements were calculated as $M_{i,j}^{a,b} = \langle x_{a,j} - \langle x_{a,i}\rangle\rangle\langle x_{b,j} - \langle x_{b,i}\rangle\rangle$, where a and b = 1, 2, or 3 represent the X, Y, or Z coordinates of Cα atoms i and j averaged over all snapshots of the last 20 ns MD trajectory as representative of equilibrium fluctuations. A transformation of the reference frame was done before calculating the matrix. In particular, we applied a roto-translation to align the frame diagonalizing the inertia tensor (calculated at each snapshot) to the origin and orientation of the frame in the first snapshot. In this way, the dynamics of the system was represented in a noninertial frame, fixed on the protein, from which only the internal dynamics was observed. The results are shown as the transformed matrix, **m**, with elements $m_{i,j} = \ln(|M_{i,j}|)$, using a cutoff of 10^{-5} for the matrix elements. This transformation is necessary to highlight the different scales of variance−covariance elements. Elements of **m** range from −11.5, corresponding to $|M_{i,j}| \leq 10^{-5}$, to $\ln(\max_{i,j}\{|M_{i,j}|\})$. The diagonal elements of matrix **m** quantify the positional constraint of single residues: high values of $m_{i,i}$ mean that Cα of residue i has high mobility. The off-diagonal terms $m_{i,j} = m_{j,i}$ quantify the spatial correlation between residues i and j: large values of $m_{i,j}$ mean that the two residues fluctuate in a

DOI: 10.1021/acs.biochem.6b00385
Biochemistry 2016, 55, 3984−3994

concerted manner so that they maintain a high degree of spatial linkage. To monitor the structural changes occurring to selected amino acids during the alchemical mutation, we applied the following analysis protocol. Before each step, i.e., incremental charge neutralization, and after the first 10 ns of the simulation of the fully mutated protein, we calculated the averaged distances among each amino acid on the ring formed by the negatively charged amino acids placed on the borders of the reaction site: Glu39, Asp60e, Glu61, Asp63, Glu97a, Glu146, Glu192, Glu217, and Asp221. Averages have been taken over the 200 ps (100 MD snapshots) preceding the next alchemical step: $d_{i,j} = \sum_{t=1}^{100} d_{i,j}(t)/100$, where i and j indexes run over the selected amino acids in both D102N and WT trajectories. Then we calculated the differences between the distances for $i-j$ amino acid pairs in D102N and WT ($\Delta d_{i,j} = d_{i,j}^{D102N} - d_{i,j}^{WT}$). For each pair, $\Delta d_{i,j}$ was graphically represented as described in Results.

Spectroscopic Measurements. Measurements were taken at 25 ± 0.1 °C in 5 mM Tris-HCl buffer (pH 8.0) containing 0.1% (w/v) PEG 8000 and 0.2 M choline chloride (ChCl). Temperature correction was applied for Tris buffer.[29] All measurements were taken in at least duplicate, and the spectra were subtracted for the corresponding baselines. The protein concentration was determined by UV absorption at 280 nm on a Lambda-2 spectrophotometer from PerkinElmer (Norwalk, CT) or Nanodrop using a molar absorptivity value of 65770 M^{-1} cm^{-1} for natural α-thrombin and mutant D102N and 2920 M^{-1} cm^{-1} for Hir(1−47). The concentration of Hir(48−64), having only one aromatic chromophore in the sequence (i.e., Phe54), was taken to be 200 M^{-1} cm^{-1} at 257 nm. The active site concentration of thrombin was also determined by titration with hirudin HM2 in the presence of FPR as a chromogenic substrate, using a procedure similar to that reported elsewhere,[30] and found to be identical (within 5% error) to that determined by UV absorption. The concentration of PABA was determined using a molar absorptivity value of 15000 M^{-1} cm^{-1} at 293 nm.[31] Far-UV CD spectra were recorded on a Jasco (Tokyo, Japan) model J-810 spectropolarimeter equipped with a water-jacketed cell holder, connected to a model RTE-111 (NesLab) water-circulating bath. The spectra were recorded in a 1 mm cell, at a scan speed of 10 nm/min, with a response time of 16 s, and resulted from the average of four accumulations. CD data were expressed as the mean of the residue ellipticity $[\theta] = \theta_{obs} \times MRW/(10lc)$, where θ_{obs} is the observed signal in degrees, MRW is the mean residue weight taken to be 114.6 Da, l is the cuvette path length in centimeters, and c is the protein concentration in grams per milliliter. Fluorescence spectra were recorded at a scan speed of 200 nm/min in a 1 cm path length cuvette (2 mL internal volume) on a Jasco model FP-6500 spectropolarimeter, equipped with Peltier model ETC-273T temperature control system from Jasco. Protein samples (5−50 nM) were excited at 280, using excitation and emission slits of 5 and 10 nm, respectively.

Stability Measurements. Urea-induced denaturation experiments were performed in 20 mM Tris-HCl buffer and 0.1% PEG 8000 (pH 8.0) at 25 ± 0.1 °C, in the presence of 0.2 M chloride salts. After a 1 h incubation at the specified urea concentration, protein samples (2 mL, 50 nM) were excited at 280 nm and the fluorescence intensity was recorded at 334 nm. At each urea concentration, the fluorescence signal was subtracted from that of the corresponding baseline. Data were analyzed within the framework of a two-state process,[32] and the value of $[urea]_{1/2}$ was estimated as described elsewhere.[33]

Binding of Ligand to Thrombin. The equilibrium association constants of Hir(1−47) and Hir(48−64) for thrombin wild type and mutant D102N were determined at 25 ± 0.1 °C in 5 mM Tris-HCl buffer (pH 8.0) containing 0.1% (w/v) PEG 8000 and the specified concentration of chloride ion by exciting the protein samples at 280 nm and measuring the increase in fluorescence intensity at 334 nm as a function of ligand concentration. Under all conditions tested, the optical density of the solution was always much lower than 0.02 unit at both λ_{ex} and λ_{em}, and therefore, no inner filter effect was observed.[34] Aliquots (2−5 μL) of ligand stock solutions were added, under gentle magnetic stirring, to a thrombin solution (5−50 nM, 2 mL) in a 1 cm path length cuvette. After being stirred for 30 s, the solution was allowed to equilibrate for 2 min, and the signal intensity was recorded at 334 nm. Fluorescence data were corrected for sample dilution, which was always lower than 2% at the end of the titration. The level of photobleaching was reduced to <2%, even after prolonged light exposure, by using a 1 cm path length quartz cuvette (2 mL internal volume) with two opaque walls that can diffuse the incident light inside the sample, thus preventing photodegradation of Trp residues. Fluorescence data were fitted to a simple one-site binding equation. For binding of Na^+ to thrombin, a solution containing 50 nM enzyme in 5 mM Tris-HCl (pH 8.0), 0.1% PEG 8000, and 400 mM NaCl was incrementally added to a solution containing 50 nM thrombin in 5 mM Tris-HCl (pH 8.0), 0.1% PEG 8000, and 400 mM ChCl. The ionic strength and enzyme concentration were held constant, while the Na^+ concentration was increased.[35] The interaction of *p*-aminobenzamidine (PABA) with thrombin was monitored by adding, under gentle magnetic stirring in a 1 cm path length cuvette, aliquots (2−10 μL) of a PABA stock solution (12.5−50 mM) to a solution of thrombin (1.4 mL, 376 nM). At each PABA concentration, the thrombin sample was equilibrated for 2 min at 25 ± 0.1 °C and excited at 325 nm, using excitation and emission slits of 5 and 10 nm, respectively. The increase in the fluorescence intensity of PABA in the presence of the enzyme was recorded at the 376 nm as a function of PABA concentration. Fluorescence data were corrected for IFE, at both λ_{ex} and λ_{em}.[34,36]

Crystallization. Crystallization of the human thrombin mutant D189A was achieved at 22 °C by the vapor diffusion technique, with 3 μL of 10 mg/mL protein mixed with 3 μL of a solution containing 200 mM KCl and 20% PEG 3350. Crystals were grown in 1−2 weeks and were cryoprotected in a solution of 200 mM KCl, 25% PEG 3350, and 20% glycerol prior to being flash-frozen. X-ray diffraction data were collected at beamline 19ID at the Advanced Photon Source (Argonne, IL) and were indexed, integrated, and scaled with the HKL2000 software package.[37] The structure was determined by molecular replacement using MOLREP from the CCP4 suite[38] and the structure of thrombin bound to PPACK (PDB entry 1SHH) as a starting model. Refinement and electron density generation were performed with REFMAC5 from the CCP4 package;[38] 5% of the reflections were randomly selected as a test set for cross-validation. Model building and analysis of the structure were conducted using COOT.[39] In the final refinement stage, TLS tensors modeling rigid-body anisotropic temperature factors were calculated and applied to the model.[40] Ramachandran plots were calculated using PROCHECK.[41] Statistics for data collection and refinement are summarized in

DOI: 10.1021/acs.biochem.6b00385
Biochemistry 2016, 55, 3984−3994

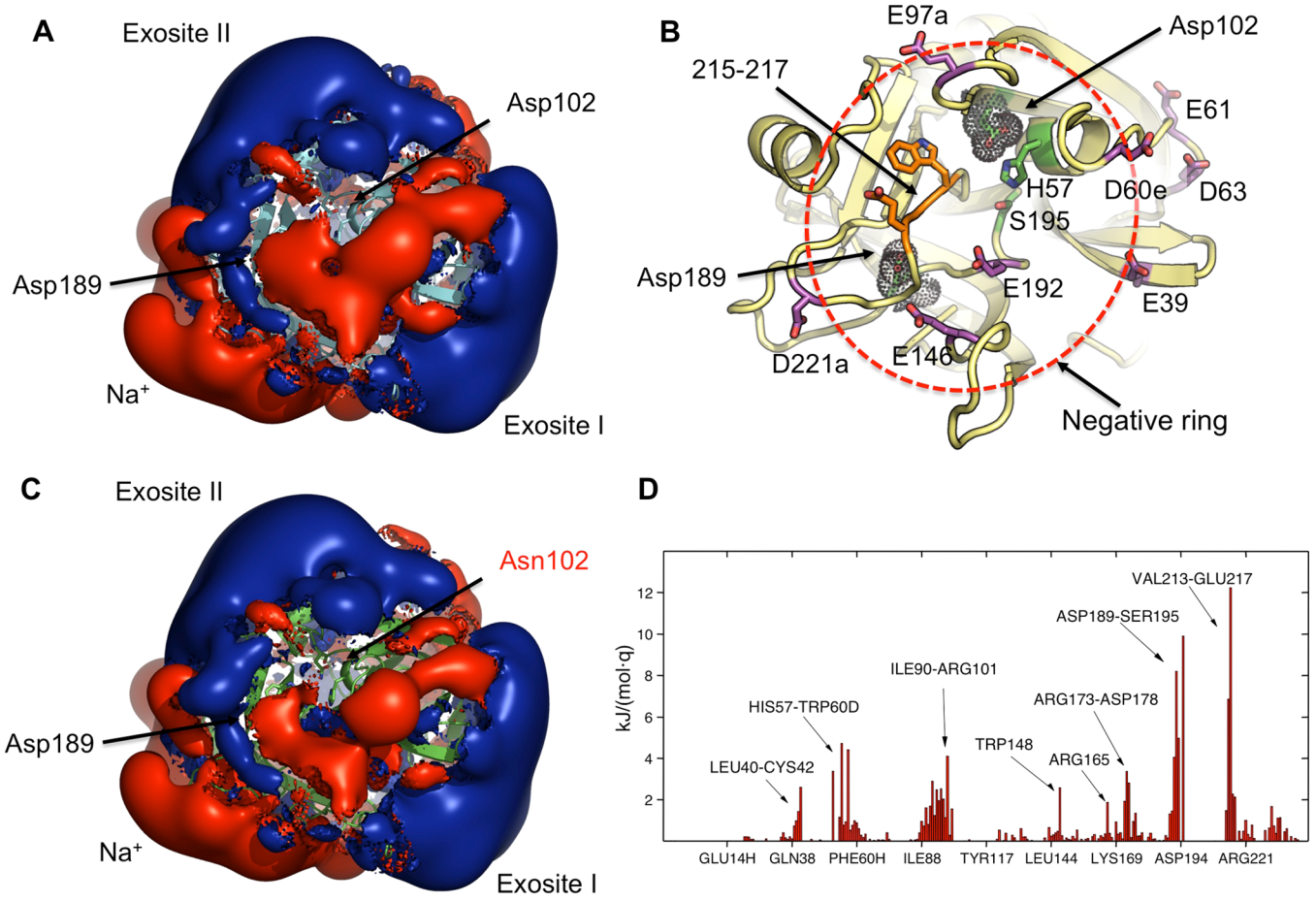

Figure 1. Negative ring surrounding the active site and electrostatic potential for (A and B) thrombin wild type and (C) D102N. (A) Strong electropositive potential (blue) dominates exosites I and II and opposes the negative potential of the Na^+ binding site (Na^+) and the active site. (B) View from the top of the active site of thrombin (1PPB). The conserved catalytic triad consists of H57, D102, and S195 (green sticks), which is located at the bottom of the active site. Movement of the 215−217 segment (orange sticks) ensures productive interaction of the incoming substrate with residue D189 (green stick) that forms the primary specificity pocket. Nine Asp and Glu residues (magenta sticks) surround the active site and generate a negative electrostatic gradient that steers positively charged substrates into the active site pocket. (C) Substitution of Asp102 with Asn weakens the electronegative potential of the active site pocket. (D) Difference in the electrostatic potential $\Delta\zeta_{(D102N-WT)}$ calculated for each residue reported as kilojoules per mole per electric charge. A positive value of $\Delta\zeta$ indicates that a given amino acid in D102N has a less negative or more positive ζ value compared to that of WT. Arrows point to protein segments that are affected by the mutation.

Table 2. Atomic coordinates and structure factors have been deposited in Protein Data Bank as entry 5JDU.

RESULTS

Electrostatics of Thrombin Wild Type and D102N. Thrombin displays a nonuniform electrostatic potential, generated by a highly asymmetric distribution of positive and negative amino acids (Figure 1A).[20] Two positively charged patches, exosite I and exosite II, oppose the active site pocket, which is negatively charged because of Asp102 and Asp189. Interestingly, this arrangement is complemented by nine Asp and Glu residues (i.e., Glu39, Asp60e, Glu61, Asp63, Glu97a, Glu146, Glu192, Glu217, and Asp221a) that form a negatively charged ring around the active site (Figure 1B). Early work on rat trypsin showed that the overall structure of mutant D102N crystallized in the presence of benzamidine could be superimposed with that of the wild type, both sharing a wide open active site primed for ligand binding.[16] However, the very same mutation in thrombin unexpectedly resulted in an occluded form of the active site due to collapse of the 215−217 segment.[15] Long-range electrostatic forces may be responsible for this conformational rearrangement. We therefore tested the hypothesis that, in thrombin, the loss of a negative charge caused by isosteric substitution of Asp with Asn may alter the electrostatic potential of regions surrounding the active site causing the 215−217 segment to reposition.

After mutating the negatively charged Asp102 to Asn in the E open form of thrombin, we calculated the electrostatic potential for the two proteins at the atomic level. Thrombin WT (Figure 1A) and D102N (Figure 1C) have similar electrostatic properties for exosite I, exosite II, and the Na^+ binding site, but substitution of Asp with Asn causes a sharp reduction of the electronegative potential around the active site. In particular, a small [$\Delta\zeta_{(D102N-WT)} < 3$ kJ mol^{-1} q^{-1}] to moderate [3 kJ mol^{-1} $q^{-1} < \Delta\zeta_{(D102N-WT)} < 6$ kJ mol^{-1} q^{-1}] change is experienced by residues Trp60d, Glu60f, Leu99, and Ile174, which are part of recognition subsites S2 and S3. Residues Leu40−Cys42, Arg173−Asp178, and Glu146−Trp148 become more positive, too. High-level perturbation [$\Delta\zeta_{(D102N-WT)} > 6$ kJ mol^{-1} q^{-1}] is seen for Asp189 and Ser195 that are 13 and 6 Å from the site of the mutation, respectively. Finally, the most significant variation

DOI: 10.1021/acs.biochem.6b00385
Biochemistry 2016, 55, 3984−3994

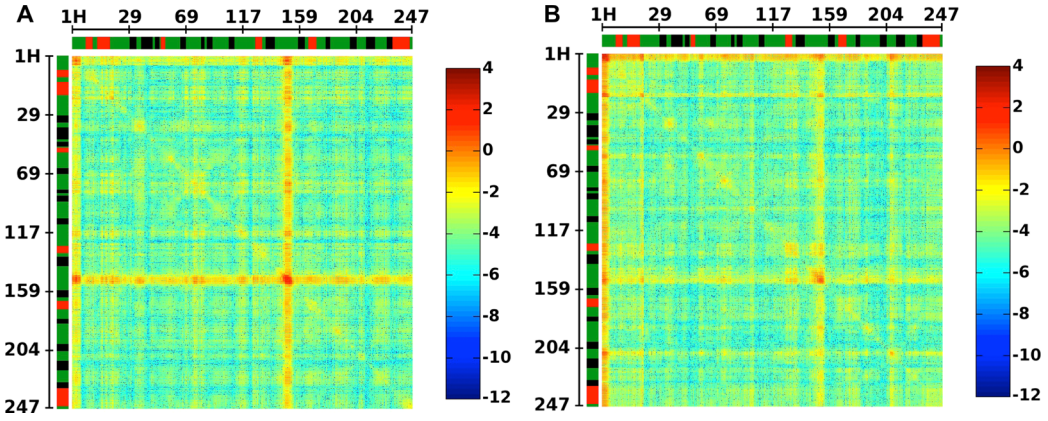

Figure 2. Transformed variance−covariance matrices, **m**, for (A) WT and (B) D102N. The transformed matrix, ***m***, with elements $m_{i,j} = \ln(|M_{i,j}|)$, was used to map the conformational flexibility profile resulting from the Asp102 to Asn mutation. The degree of variance−covariance is color-coded; no variance−covariance is shown as dark blue, and high variance−covariance is shown as dark red. The numbering follows the chymotrypsinogen scheme, and the secondary structure elements are reported as follows: α-helices in red, β-sheets in black, and loops and random coils in green. The most striking difference concerns the 141−155 segment, which is centered on residue Gly149e in the autolysis loop. In the wild type (A), this segment is strongly correlated with all other residues of the protein (intense red cross) but this spatial correlation is lost upon mutation.

strikes the 213−217 strand where $\Delta\zeta$ reaches a value of 12.5 kJ mol^{-1} q^{-1}.

Molecular Dynamics Simulations. All-atom MD simulations were performed on the E forms of WT and D102N to improve our understanding of the structural consequences of this perturbation. Overall, the mutation does not change the tertiary or secondary structure of the enzyme, as expected.[15] The effect is rather local; it affects flexible loops and overlaps with regions identified previously by our electrostatic calculations. Relevant to the catalytic mechanism, His57 shows an enhanced flexibility in the mutant. This is due to a different protonation state of Nε2. The altered protonation state results in increased mobility of Ser195. Residue Arg221a, whose carbonyl oxygen offers hydrogen bonding to coordinate Na^+, shows a much higher root-mean-square deviation (rmsd) upon mutation, from 0.17 to 0.35 nm. The larger conformational space explored by the side chain of Arg221a in the D102N structure makes the formation of such an interaction unlikely. Relevant to the E*−E conformational equilibrium, the side chains of Trp60d, Trp148, and Trp215 experience similar or lower dynamics but on average assume a position closer to the catalytic triad. Some differences are also notable in the N-terminal region, but the high rmsd in both protein systems discourages facile conclusions. A more comprehensive view of the structural and dynamic changes introduced by the mutation comes from analysis of the variance−covariance matrix obtained by averaging the MD trajectories over the last 20 ns of the simulation (Figure 2). Thrombin WT and D102N show similar magnitudes of the diagonal elements, indicating unaltered backbone flexibility upon mutation. On the other hand, the magnitude of most of the out-of-diagonal elements is reduced in D102N, suggesting that the spatial correlation between residues has been weakened by the mutation. This effect is particularly evident for the 141−155 segment linking the flexible autolysis loop to the E*−E equilibrium. Indeed, deletion of nine residues of this loop, ^{146}ETWTANVGK^{149e}, stabilizes thrombin in the E* form,[42] whereas replacement of the autolysis loop with the homologous loop of the murine enzyme, ^{146}ETWTTNINEI^{150}, results in a significant improvement in catalytic activity via stabilization of the E form.[43] The deletion Δ146−149e eliminates one negative charge, Glu146, which is part of the outer ring. On the other hand, in the murine to human swap, the replacement of ^{149d}GKG^{150} with ^{149d}NEI^{150} rigidifies the loop and inverts the charge ratio of the polypeptide sequence from +1 to −1, increasing the extent of electrostatic repulsion.

Further insights into the role of Asp102 come from simulations in which the negative charge on the carboxylate group was gradually turned off before substitution of Asp with Asn. When one moves from panel A (−0.75) to panel D (0) to panel E (-NH_2) of Figure 3, there is an almost complete reversal of the colors for residues Glu192, Trp215, Glu217, and Asp221, from blue to red. Residue Glu146 goes from red to blue. Of note, residues Glu192, Trp215, Glu217, and Asp221 move toward Tyr60a and Trp60d in the 60-loop, which is located on the opposite side of the active site pocket. This movement is expected to narrow the aperture of the active site, thereby decreasing the docking efficiency of any ligand. Considering the solvent accessible surface area (SASA) of the active site pocket, an appropriate structural marker of the occlusion, we continuously monitored its fluctuation during the simulations. Results are shown in Figure 3F. From step 1 to 3, i.e., Asp(−0.75), Asp(−0.5), and Asp(−0.25), $SASA^{D102N}$ remains on average similar to $SASA^{WT}$. In the penultimate step, when the charge is completely annihilated, the two traces start to differentiate, with $SASA^{D102N}$ becoming lower than $SASA^{WT}$. The same trend continues after Asp(0) is mutated to Asn. Interestingly, there is a drop at 50 ns in the trace of the mutant. However, this is a transient state and not statistically significant. In fact, the system rapidly relaxes and stabilizes to an average SASA of 1050 $Å^2$, which is the center of the Gaussian distribution of the values of $SASA^{D102N}$ obtained over the trajectory of the last 50 ns of the simulations. On average, $SASA^{D102N}$ is 100 $Å^2$ smaller than $SASA^{WT}$, and this is due to the movement of residues 192, 215, 217, and 221 toward the 60-loop. Remarkably, the charge annihilation of Asp102 is necessary and sufficient to trigger the conformational transition in thrombin. Substitution of the hydroxyl group with an amine simply completes the stabilization by offering perhaps a favorable environment for forming hydrogen bonds.

Spectroscopic Studies. The solution properties of D102N were investigated by circular dichroism (CD) and fluorescence spectroscopy and compared to those of WT (Figure 4A,B). In

DOI: 10.1021/acs.biochem.6b00385
Biochemistry 2016, 55, 3984−3994

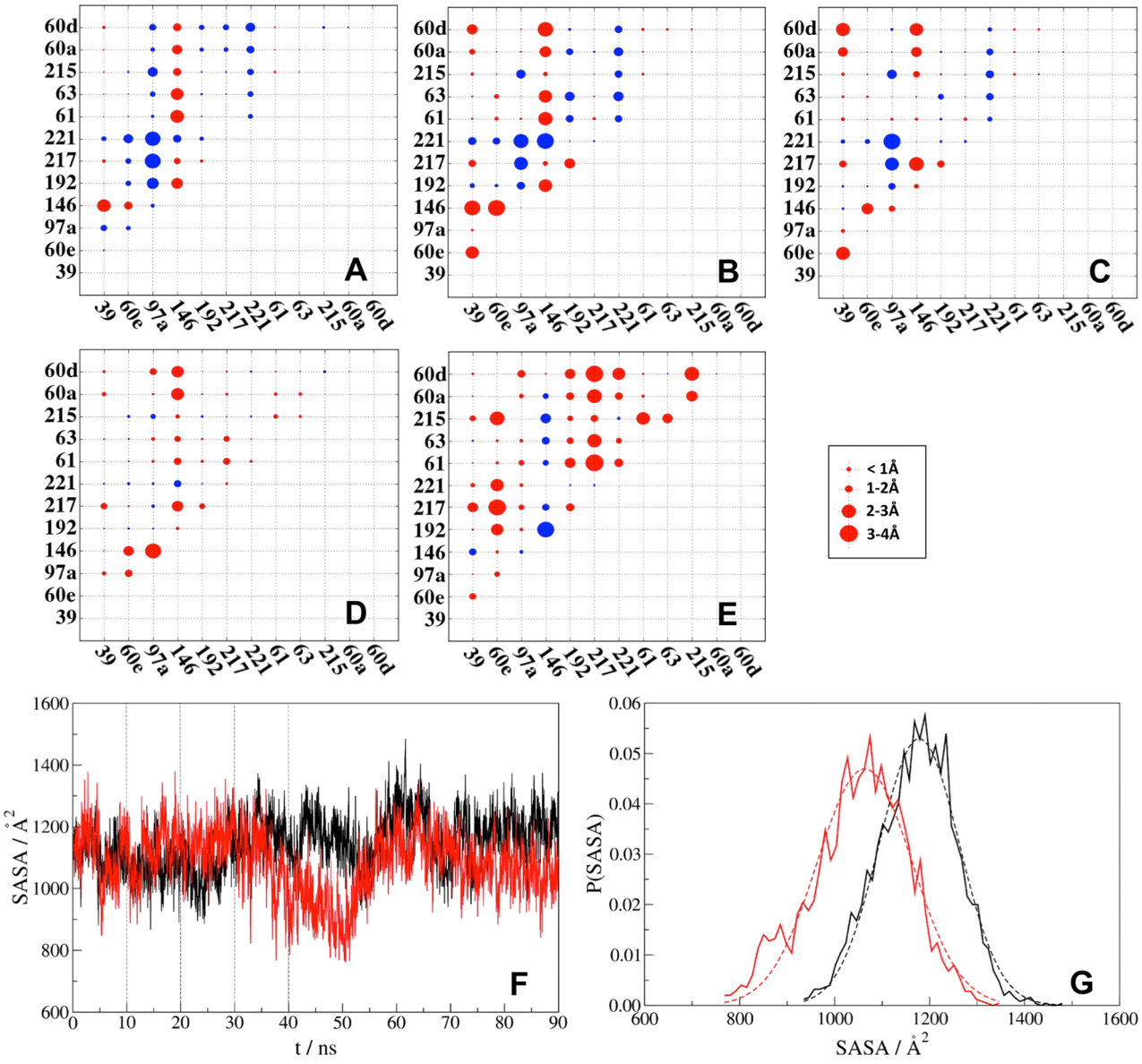

Figure 3. Alchemical mutation. Variation ($\Delta d_{i,j}$) of selected residues for each alchemical step: (A) −0.75, (B) −0.5, (C) −0.25, (D), 0, and (E) Asn. The distance between a pair of residues (i,j) was calculated for the wild type ($d_{i,j}^{WT}$) in each step of the simulation and then subtracted from the distance of the same pair calculated in the D102N ($d_{i,j}^{D102N}$). The difference between these two quantities ($\Delta d_{i,j} = d_{i,j}^{D102N} - d_{i,j}^{WT}$) was used to visualize structural changes for those residues whose electrostatic potential was affected by the mutation. The dimension of the circle located at the intersection of each quadrant directly informs on the magnitude and sign of the vector associated with $\Delta d_{i,j}$. When two amino acids i and j are closer in D102N than in WT, $\Delta d_{i,j} < 0$ and the circle is colored red. On the other hand, when $\Delta d_{i,j} > 0$, the circle is colored blue. (F) Evolution of the solvent accessible surface area (SASA) of the active site pocket identified using CASTp for wild type (black) and D102N (red). Vertical dashed lines mark the end of each step of the alchemical mutation. (G) SASA distribution [P(SASA)] for thrombin WT (black) and D102N (red) fitted to a single Gaussian function.

the free form (0.2 M ChCl), thrombin wild type has a very distinguishing far-UV CD spectrum characterized by a shallow transition between the two minima located at 208 and 225 nm.[44] The far-UV CD spectrum of D102N differs in both shape and intensity. The first minimum at 208 nm is conserved, whereas the second minimum shifts 4 nm to the right, from 225 to 229 nm. The transition between these two new minima is sharp and reaches a maximum at 220 nm. Although the shape of this spectrum may recall profiles obtained for α-helix-containing peptides, both the intensity and position of the minima are not compatible with such secondary structure. Instead, the spectrum of thrombin is dominated by the contribution of 31 aromatic amino acids (11 Phe, 9 Trp, and 11 Tyr residues).[44] The predominance of these residues is why the movement of the 215−217 segment in D102N, and in particular relocation of the side chain of Trp215 into the active site, leads to such a different far-UV CD spectrum. Similarly, the more hydrophobic environment experienced by some aromatic residues explains why there is a small but significant increase (6%) in the fluorescence quantum yield (Figure 4B).[34] Assuming a collapsed conformation for the mutant D102N, we would also expect a higher resistance to chemical denaturation. Because chemicals must diffuse into the protein core to promote unfolding, disordered and flexible proteins typically require a lower denaturant concentration to unfold, whereas globular and compact proteins are generally more stable. In our

DOI: 10.1021/acs.biochem.6b00385
Biochemistry 2016, 55, 3984−3994

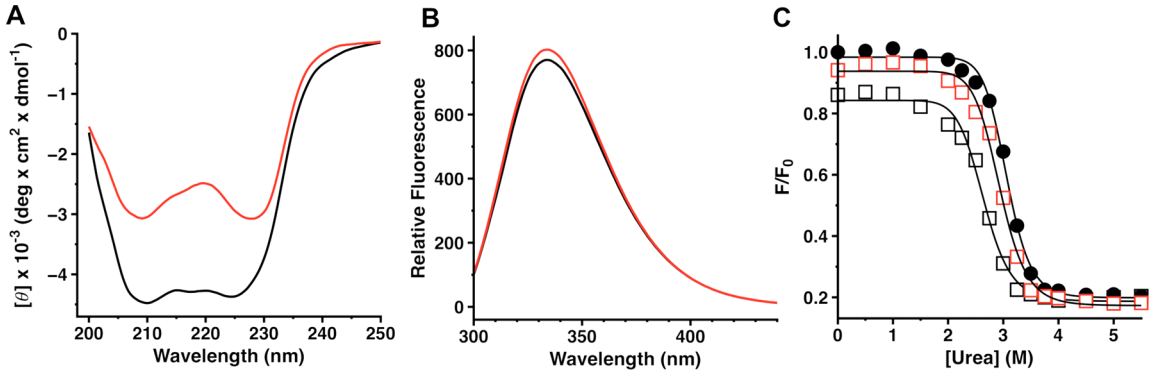

Figure 4. Spectroscopic studies. (A) Far-UV CD and (B) fluorescence spectra of thrombin wild type (black) and D102N (red). (C) Urea-induced denaturation experiments were performed at a protein concentration of 50 nM by following the decrease in fluorescence intensity at 334 nm after excitation at 280 nm. Data are reported as F/F_0, where F is the fluorescence intensity at any given concentration of urea and F_0 is the intensity of thrombin wild type at pH 8.0 in 200 mM NaCl. Experimental conditions: 20 mM Tris-HCl buffer (pH 8.0), 0.1% PEG 8000, and 200 mM NaCl (●) or 200 mM ChCl (□). The values of $[\text{urea}]_{1/2}$ extrapolated from the fit are 2.6 ± 0.1 M for WT_{ChCl}, 3.2 ± 0.1 M for WT_{NaCl}, and 3.1 ± 0.1 M for $D102N_{ChCl}$.

Table 1. Equilibrium Dissociation Constants (micromolar) for Compounds that Bind to the Active Site and Exosite I of Thrombin Wild Type and Mutant D102N[a]

	WT		D102N	
	NaCl	ChCl	NaCl	ChCl
PABA	49 ± 2	182 ± 5	354 ± 9	>10000
Hir(1−47)	0.040 ± 0.002	1.44 ± 0.02	5.2 ± 0.2	>150
Hir(48−64)	2.3 ± 0.3[b]	8.1 ± 0.3	2.2 ± 0.3	19.3 ± 0.9
Hir(1−47) and Hir(48−64)	0.037 ± 0.002	0.14 ± 0.01	2.9 ± 0.1	>120

[a]Experimental conditions: 5 mM Tris and 0.1% PEG 8000 (pH 8.0) at 25 °C. The ionic strength was kept constant at 200 or 800 mM with ChCl. When the fluorescence signal was too weak to describe a titration curve, only the lower limit for the K_d was extrapolated from the fit. [b]No fluorescence change was detected upon binding of fragment Hir(48−64) to thrombin wild type in the presence of NaCl because saturation of Na^+ binding site causes a similar fluorescence.[58] This value is from ref 50.

experiments, the fluorescence intensity at λ_{max} was monitored while the concentration of urea was being increased (Figure 4C).[32,44,45] In both proteins, the curves followed a single sharp transition, suggestive of a highly cooperative unfolding process. The concentration of urea that unfolds 50% of the protein, i.e., $[\text{urea}]_{1/2}$, was then used to compare the stability of thrombin wild type and D102N. Under all the experimental conditions tested, the mutant was more resistant to chemical denaturation, displaying a $[\text{urea}]_{1/2}$ value of 3.1 ± 0.1 M, which is 0.5 M higher than that of the wild type in the free form but similar to that of the Na^+-bound form of thrombin ($E:Na^+$).

Binding of Ligand to Thrombin Wild Type and D102N. Conclusive evidence that mutation of Asp102 to Asn shifts the conformational equilibrium toward the E* form of thrombin comes from binding studies aimed at probing the accessibility of the active site, i.e., PABA and Hir(1−47), exosite I, i.e., Hir(48−64), and Na^+ binding site (Table 1 and Figure 5A−D). As expected, in the free form, D102N binds weakly to PABA (>10 mM) (Figure 6A) and Hir(1−47) (>150 μM) (Figure 6B). The affinity for Na^+ is also compromised (Figure 5C) and decreases 6-fold, from 18 ± 1 mM in the wild type to 120 ± 5 mM in the mutant. In contrast, binding of the C-terminal fragment of hirudin Hir(48−64) is minimally affected by the mutation (Figure 5D). Na^+ is an allosteric activator of thrombin,[46,47] and it is well established that positive linkage exists between Na^+ binding and the transition to the E form.[48] This property is conserved upon mutation. In the presence of 0.8 M NaCl, PABA binds to D102N with an affinity constant of 354 ± 9 μM, which is similar to the value of 182 ± 5 μM for thrombin wild type in the free form and only 7-fold lower than that in the $E:Na^+$ form. Similar results were obtained with the N-terminal fragment of hirudin Hir(1−47). Titration of Na^+ (Figure 5B) progressively rescues the opening of the active site, and the affinity for Hir(1−47) at 0.8 M NaCl is 5.2 μM, which is only 4 times lower than that of the wild type in ChCl, i.e., 1.4 μM but still 150-fold worse compared to that of the $E:Na^+$-bound form of the wild type. The difference between PABA and Hir(1−47) requires attention. Both ligands bind to the active site but interact with different subsites that do not overlap. PABA binds to D189 in the primary specificity pocket,[31] and its ability to penetrate the active site is dominated by diffusion. Hir(1−47) engages multiple subsites, including S2 and S3,[19,49] whose conformational dynamics are likely affected independently by the adjacent mutation and not linked to Na^+ binding. This would explain why under almost saturating concentrations of Na^+, the affinity for the larger Hir(1−47) is more compromised than that of the smaller PABA. Another class of a physiological allosteric activator of thrombin includes molecules that bind to exosite I such as Hir(48−64).[50,51] In the presence of saturating concentrations of Hir(48−64), the affinity for Hir(1−47) increases 10-fold, from 1.4 μM to 140 nM, and becomes similar to the affinity of Hir(1−47) obtained in the presence of Na^+, i.e., 40 nM. Unexpectedly, this enhancement is not seen in the mutant (Figure 6A). Saturating concentrations of Hir(48−64) slightly improve the affinity of Hir(1−47) but are not enough to shift the equilibrium toward a conformation of the enzyme that is fully competent for binding. This can be achieved with minimal concentrations of Na^+, i.e., 5

DOI: 10.1021/acs.biochem.6b00385
Biochemistry 2016, 55, 3984−3994

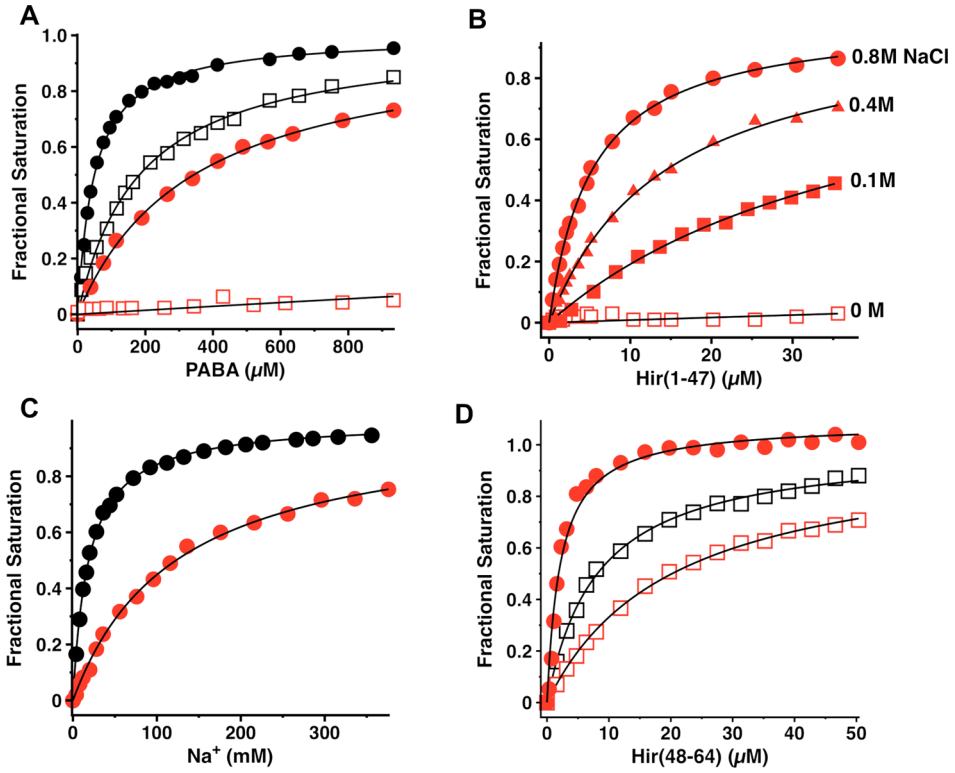

Figure 5. Binding of ligand to thrombin wild type and D102N. Equilibrium binding curves for binding of (A) PABA, (B) Hir(1−47), (C) Na^+, and (D) Hir(48−64) to thrombin wild type (black) and D102N (red). Data are presented as fractional saturation according to the normalization $(F - F_0)/\Delta F_{max}$, where F_0 is the fluorescence intensity without ligand and F_{max} is the fluorescence intensity at a saturating concentration of ligand extrapolated from the fit. Solid lines were drawn according to a simple binding equation with best fit parameters listed in Table 1. Experimental conditions: 5 mM Tris-HCl (pH 8.0), 0.1% PEG 8000, and 800 mM NaCl (filled circles) or ChCl (empty squares) for PABA and Hir(48−64) and 5 mM Tris-HCl (pH 8.0), 0.1% PEG 8000, and 0−800 mM NaCl for Hir(1−47). The ionic strength was kept constant with ChCl.

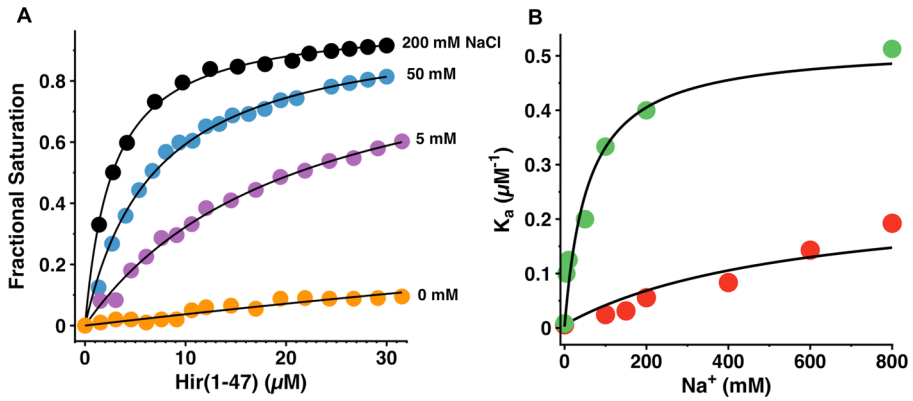

Figure 6. Linkage among Na^+, the active site, and exosite I. (A) Equilibrium binding curves for binding of Hir(1−47) to thrombin D102N at saturating concentrations of Hir(48−64) and different concentrations of Na^+. (B) Linkage between Na^+ and Hir(1−47) binding to D102N in the absence (red circles) and presence (green circles) of a saturating concentration of Hir(48−64). Shown is the effect of a saturating concentration of Hir(48−64) (200 μM) on the equilibrium association constants for the binding of Hir(1−47) to thrombin D102N. Solid lines were drawn according to the linkage equation $K_a = [K_a^0 + K_a^1([Na^+]/K_d)]/(1 + [Na^+]/K_d)$, where K_a^0 and K_a^1 are the values of K_a for Hir(1−47) binding in the absence of Na^+ and at a saturating concentration of Na^+, respectively, and K_d is the equilibrium dissociation constant for Na^+. Best fit parameter values are as follows: for Hir(1−47), $K_a^0 = 5.7 \times 10^3\ M^{-1}$ (fixed), $K_a^1 = 2.5 \times 10^5\ M^{-1}$ (fixed), and $K_d(Na^+) = 578$ mM; for Hir(1−47) and Hir(48−64), $K_a^0 = 8.3 \times 10^3\ M^{-1}$ (fixed), $K_a^1 = 5.1 \times 10^5\ M^{-1}$, and $K_d(Na^+) = 57 \pm 10$ mM. Experimental conditions: 5 mM Tris-HCl (pH 8.0) and 0.1% PEG 8000 at 25 °C.

mM, suggesting that (1) Na^+ is necessary to change the distribution between E* and E forms of the enzyme and (2) a strong coupling between exosite I and the Na^+ binding site must exist. Indeed, Hir(48−64) improves 10-fold the affinity for Na^+, which was measured from the effect of linkage on Hir(1−47) binding (Figure 6B).[52,53]

Crystal Structure of Thrombin D189A. The proposed electrostatic model of thrombin also predicts that removal of the negatively charged Asp189 would favor collapse of the 215−217 segment. Replacement of Asp189 with Ala, Asn, Glu, or Ser compromises the specificity of thrombin toward synthetic and physiological substrates by up to 4 orders of

DOI: 10.1021/acs.biochem.6b00385
Biochemistry 2016, 55, 3984−3994

magnitude, and mutants D189A and D189N share comparable functional properties.[17] The X-ray crystal structure of the thrombin mutant D189A was determined at 1.7 Å resolution in the free form, in the absence of any ligands (Table 2). The asymmetric unit contains two molecules that overlap with an rmsd of 0.204 Å. The high resolution allowed us to assign with confidence the site of mutation, but not the 144−152 segment in the flexible autolysis loop. As predicted, D189A crystallizes in the E* form. Strands 215−217 and 190−193 connected by the Cys191−Cys220 disulfide bond collapse into the active site. The Cα−Cα distance between Gly216 and Gly193 is only 7.9 Å, as expected for the E* form (Figure 7).[6,9] In this conformation, substrate cannot penetrate the primary specificity pocket. The same Cα−Cα distance increases from 7.9 to 12.1 Å upon transition to the E form or binding of PPACK. Perturbation of the electrostatic potential caused by substituting Asp102 with Asn and Asp189 with Ala turns thrombin into E*.

Table 2. Crystallographic Data for Human Thrombin Mutant D189A

buffer/salt	200 mM KCl
PEG	3350 (20%)
Data Collection	
wavelength (Å)	0.90
space group	$P2_12_12_1$
unit cell dimensions (Å)	a = 55.4, b = 81.3, c = 146.4
no. of molecules per asymmetric unit	2
resolution range (Å)	40−1.7
no. of observations	626477
no. of unique observations	74112
completeness (%)	99.9 (99.8)
R_{sym} (%)	10.5 (39.4)
$I/\sigma(I)$	18.2 (3.2)
Refinement	
resolution (Å)	40−1.7
$\|F\|/\sigma(\|F\|)$	no cutoff
R_{cryst}, R_{free}	0.181, 0.206
no. of reflections (working/test)	70070/3729
no. of protein atoms	4473
no. of NAG/Cl^-	4/1
no. of solvent molecules	622
rmsd for bond lengths[a] (Å)	0.011
rmsd for bond angles[a] (deg)	1.4
rmsd for DB (Å^2) (mm/ms/ss)[b]	1.85/1.44/2.73
⟨B⟩ for protein (Å^2)	26.3
⟨B⟩ for NAG/Cl^- (Å^2)	44.5/24.0
⟨B⟩ for solvent (Å^2)	37.9
Ramachandran plot (%)	
most favored	99.6
generously allowed	0.0
disallowed	0.4

[a]Root-mean-squared deviation from ideal bond lengths and angles. [b]Root-mean-squared deviation in B factors of bonded atoms. Legend: mm, main chain−main chain; ms, main chain−side chain; ss, side chain−side chain.

DISCUSSION

Recent analysis of the Protein Data Bank has shown that trypsin-like proteases exist in closed (E*) and open (E) forms at equilibrium and points to the 215−217 segment as the gatekeeper of the active site.[6] A high-resolution structure of chymotrypsinogen was the first to reveal two distinct conformations of the 215−217 segment in two molecules in the asymmetric unit, consistent with the E*−E equilibrium.[54] More recently, thrombin mutants Y225P and N143P have been trapped in alternative forms with open and closed conformations of the active site.[5,55]

In this study, we offer compelling evidence as to why mutation of Asp102 or Asp189 leads to a dramatic structural rearrangement and stabilization of the E* form and propose a model that explains the results from previous studies. The active site pocket of thrombin can be represented as a funnel in which Asp102 in the catalytic site and Asp189 in the primary specificity site are positioned below a negative ring surrounding the active site (Figure 1B). It is therefore conceivable that neutralization of Asp102 and Asp189 could lead to a rearrangement of the electrostatic potential. Electrostatics, molecular dynamics simulations, and structural biology point to the 215−217 strand as the structural element that is the most affected by the charge neutralization and show how the active site pocket becomes stabilized into a collapsed conformation incapable of ligand binding.

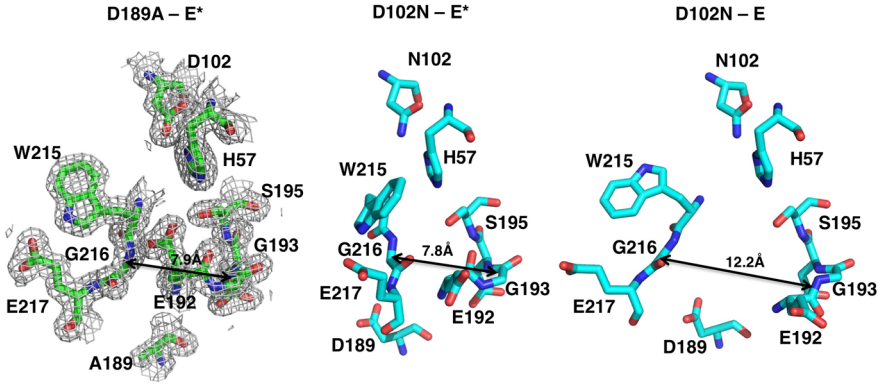

Figure 7. Crystal structure of thrombin D189A. X-ray crystal structure of thrombin mutant D189A compared to that of D102N free (E*, 2GP9) and D102N bound to the extracellular fragment of PAR-1 (EL, 3BEF). Thrombin D189A crystallizes in the E* form. The electron density is shown as the $2F_o - F_c$ map contoured at 1σ. The Cα−Cα distance between G216 and G193 is 7.9 Å. Such a distance is conserved in the crystal structures of D102N,[15] Y225P,[5] N143P,[55] Δ146−149e,[42] and E217K[56] and thus is a hallmark of the E* conformation in thrombin. E and EL structures require a wider aperture, 12.2 Å, to accommodate any ligand.

DOI: 10.1021/acs.biochem.6b00385
Biochemistry 2016, 55, 3984−3994

Structural highlights of the E* forms are the collapse of the 215−217 segment to occlude the active site, increased flexibility of residue Arg221a that can be found either exposed to the solvent or pointing toward the protein core occupying the primary specificity pocket, and relocation or disorder of the residues in the 186-loop forming the Na^+ binding site.[5,6,15,56] In these conformations, thrombin would not be able to bind active site ligands such as PABA or the N-terminal fragment of hirudin Hir(1−47) as well as Na^+. In agreement with structural biology, D102N binds weakly to PABA and the N-terminal fragment of hirudin Hir(1−47) and the affinity for Na^+ is compromised. Positive linkage exists between the Na^+ binding site and the opening of the active site as well as exosite I and the Na^+ binding site, as expected from rapid kinetics and structural biology.[48,55] Interestingly, the coupling between exosite I and the active site is weakened by the mutation. In the wild type, binding to exosite I favors more active conformers within the E ensemble without affecting significantly the E*−E distribution.[9] Because D102N mostly exists in the E* form, the effect of hirugen is small because of the reduced population of E, which has been trapped in the crystal structure of D102N bound to the fragment of the protease-activated receptor PAR-1.[57]

Further insight into the conformational and dynamic properties of E* in solution comes from spectroscopic studies. The far-UV CD and fluorescence spectra of D102N are different compared to that of WT and reflect the enrichment of E* caused by the mutation. The stability studies show that the E* form of thrombin, as represented by the mutant D102N, may be thermodynamically favored with respect to the E form but not the E:Na^+ form. This defines an energy landscape in which the E form is an intermediate between E*- and E-bound forms of the enzyme. The negative charge of Asp102 and Asp189 therefore has a structural role because it reduces the probability of thrombin being in the collapsed form.

■ ASSOCIATED CONTENT

Supporting Information

The Supporting Information is available free of charge on the ACS Publications website at DOI: 10.1021/acs.biochem.6b00385.

Carbohydrate chain connected to residue Asn60g of thrombin (Figure S1) and schematic protocol employed for the alchemical morphing of Asp102 into Asn102 (Figure S2) (PDF)

■ AUTHOR INFORMATION

Corresponding Authors

*Department of Biochemistry and Molecular Biology, Saint Louis University School of Medicine, St. Louis, MO 63104. E-email: npozzi@slu.edu. Telephone: (314) 977-9257. Fax: (314) 977-9206.

*Department of Biochemistry and Molecular Biology, Saint Louis University School of Medicine, St. Louis, MO 63104. E-email: enrico@slu.edu. Telephone: (314) 977-9201. Fax: (314) 977-9206.

*Department of Pharmaceutical Sciences, University of Padua, Padua, Italy 35131. E-email: vincenzo.defilippis@unipd.it. Telephone: +39-049-827-5698. Fax: +39-049-827-5366.

Author Contributions

V.D.F., M.Z., D.F., and N.P. designed the research. N.P., M.Z., D.F., L.A., S.T., and D.W.G. performed the research. N.P., M.Z., D.F., D.W.G., E.D.C., and V.D.F. analyzed the results. N.P., M.Z., D.F., A.P., E.D.C., and V.D.F. wrote the manuscript. All authors reviewed the content of the manuscript.

Funding

This work was supported in part by the M3PC Grant from the CARIPARO Foundation Excellence Research Project to A.P., a Grant from the American Heart Association 15SDG25550094 to N.P., and National Institutes of Health Research Grants HL049413, HL073813, and HL112303 to E.D.C.

Notes

The authors declare no competing financial interest.

■ ACKNOWLEDGMENTS

We are grateful to Ms. Tracey Baird for help with illustrations, Leslie A. Pelc for proofreading the manuscript, Chris Carrell for his help with the crystallization of D189A, and Zhiwei Chen for depositing the coordinates of thrombin mutant D189A with the PDB. Molecular dynamics simulations have been run on the C3P ("Centro di Chimica Computazionale di Padova") HPC facility of the Department of Chemical Sciences at the University of Padua.

■ REFERENCES

(1) Page, M. J., and Di Cera, E. (2008) Serine peptidases: classification, structure and function. *Cell. Mol. Life Sci. 65*, 1220−1236.

(2) Hedstrom, L. (2002) An overview of serine proteases. *Current Protocols in Protein Science*, Chapter 21, unit 21, 10, Wiley, New York.

(3) Hedstrom, L. (2002) Serine protease mechanism and specificity. *Chem. Rev. 102*, 4501−4524.

(4) Di Cera, E. (2008) Thrombin. *Mol. Aspects Med. 29*, 203−254.

(5) Niu, W., Chen, Z., Gandhi, P. S., Vogt, A. D., Pozzi, N., Pelc, L. A., Zapata, F., and Di Cera, E. (2011) Crystallographic and Kinetic Evidence of Allostery in a Trypsin-like Protease. *Biochemistry 50*, 6301−6307.

(6) Pozzi, N., Vogt, A. D., Gohara, D. W., and Di Cera, E. (2012) Conformational selection in trypsin-like proteases. *Curr. Opin. Struct. Biol. 22*, 421−431.

(7) Vogt, A. D., and Di Cera, E. (2013) Conformational selection is a dominant mechanism of ligand binding. *Biochemistry 52*, 5723−5729.

(8) Vogt, A. D., and Di Cera, E. (2012) Conformational selection or induced fit? A critical appraisal of the kinetic mechanism. *Biochemistry 51*, 5894−5902.

(9) Vogt, A. D., Chakraborty, P., and Di Cera, E. (2015) Kinetic dissection of the pre-existing conformational equilibrium in the trypsin fold. *J. Biol. Chem. 290*, 22435−22445.

(10) Lechtenberg, B. C., Johnson, D. J., Freund, S. M., and Huntington, J. A. (2010) NMR resonance assignments of thrombin reveal the conformational and dynamic effects of ligation. *Proc. Natl. Acad. Sci. U. S. A. 107*, 14087−14092.

(11) Fuglestad, B., Gasper, P. M., McCammon, J. A., Markwick, P. R., and Komives, E. A. (2013) Correlated motions and residual frustration in thrombin. *J. Phys. Chem. B 117*, 12857−12863.

(12) Fuglestad, B., Gasper, P. M., Tonelli, M., McCammon, J. A., Markwick, P. R., and Komives, E. A. (2012) The dynamic structure of thrombin in solution. *Biophys. J. 103*, 79−88.

(13) Plattner, N., and Noe, F. (2015) Protein conformational plasticity and complex ligand-binding kinetics explored by atomistic simulations and Markov models. *Nat. Commun. 6*, 7653.

(14) Pelc, L. A., Chen, Z., Gohara, D. W., Vogt, A. D., Pozzi, N., and Di Cera, E. (2015) Why Ser. and not Thr brokers catalysis in the trypsin fold. *Biochemistry 54*, 1457−1464.

(15) Pineda, A. O., Chen, Z. W., Bah, A., Garvey, L. C., Mathews, F. S., and Di Cera, E. (2006) Crystal structure of thrombin in a self-inhibited conformation. *J. Biol. Chem. 281*, 32922−32928.

(16) Sprang, S., Standing, T., Fletterick, R. J., Stroud, R. M., Finer-Moore, J., Xuong, N. H., Hamlin, R., Rutter, W. J., and Craik, C. S.

DOI: 10.1021/acs.biochem.6b00385
Biochemistry 2016, 55, 3984−3994

(1987) The three-dimensional structure of Asn102 mutant of trypsin: role of Asp102 in serine protease catalysis. *Science 237*, 905−909.
(17) Prasad, S., Cantwell, A. M., Bush, L. A., Shih, P., Xu, H., and Di Cera, E. (2004) Residue Asp-189 controls both substrate binding and the monovalent cation specificity of thrombin. *J. Biol. Chem. 279*, 10103−10108.
(18) Pozzi, N., Chen, Z., Pelc, L. A., Shropshire, D. B., and Di Cera, E. (2014) The linker connecting the two kringles plays a key role in prothrombin activation. *Proc. Natl. Acad. Sci. U. S. A. 111*, 7630−7635.
(19) De Filippis, V., Colombo, G., Russo, I., Spadari, B., and Fontana, A. (2002) Probing the hirudin-thrombin interaction by incorporation of noncoded amino acids and molecular dynamics simulation. *Biochemistry 41*, 13556−13569.
(20) Bode, W., Mayr, I., Baumann, U., Huber, R., Stone, S. R., and Hofsteenge, J. (1989) The refined 1.9 A crystal structure of human alpha-thrombin: interaction with D-Phe-Pro-Arg chloromethylketone and significance of the Tyr-Pro-Pro-Trp insertion segment. *EMBO J. 8*, 3467−3475.
(21) Baker, N. A., Sept, D., Joseph, S., Holst, M. J., and McCammon, J. A. (2001) Electrostatics of nanosystems: application to microtubules and the ribosome. *Proc. Natl. Acad. Sci. U. S. A. 98*, 10037−10041.
(22) Fogolari, F., Corazza, A., Yarra, V., Jalaru, A., Viglino, P., and Esposito, G. (2012) Bluues: a program for the analysis of the electrostatic properties of proteins based on generalized Born radii. *BMC Bioinf. 13* (Suppl. 4), S18.
(23) Bashford, D., and Case, D. A. (2000) Generalized born models of macromolecular solvation effects. *Annu. Rev. Phys. Chem. 51*, 129−152.
(24) Nilsson, B., Horne, M. K., 3rd, and Gralnick, H. R. (1983) The carbohydrate of human thrombin: structural analysis of glycoprotein oligosaccharides by mass spectrometry. *Arch. Biochem. Biophys. 224*, 127−133.
(25) Foloppe, N., and MacKerell, A. D., Jr. (2000) All-atom empirical force field for nucleic acids: I. Parameter optimization based on small molecule and condensed phase macromolecular target data. *J. Comput. Chem. 21*, 86−104.
(26) Kuttel, M., Brady, J. W., and Naidoo, K. J. (2002) Carbohydrate solution simulations: producing a force field with experimentally consistent primary alcohol rotational frequencies and populations. *J. Comput. Chem. 23*, 1236−1243.
(27) Nielsen, J. E. (2007) Analysing the pH-dependent properties of proteins using pKa calculations. *J. Mol. Graphics Modell. 25*, 691−699.
(28) Phillips, J. C., Braun, R., Wang, W., Gumbart, J., Tajkhorshid, E., Villa, E., Chipot, C., Skeel, R. D., Kale, L., and Schulten, K. (2005) Scalable molecular dynamics with NAMD. *J. Comput. Chem. 26*, 1781−1802.
(29) Stoll, V. S., and Blanchard, J. S. (1990) Buffers: principles and practice. *Methods Enzymol. 182*, 24−38.
(30) Dang, Q. D., and Di Cera, E. (1994) A simple activity assay for thrombin and hirudin. *J. Protein Chem. 13*, 367−373.
(31) Evans, S. A., Olson, S. T., and Shore, J. D. (1982) p-Aminobenzamidine as a fluorescent probe for the active site of serine proteases. *J. Biol. Chem. 257*, 3014−3017.
(32) Eftink, M. R. (1994) The use of fluorescence methods to monitor unfolding transitions in proteins. *Biophys. J. 66*, 482−501.
(33) Di Stasio, E., Bizzarri, P., Misiti, F., Pavoni, E., and Brancaccio, A. (2004) A fast and accurate procedure to collect and analyze unfolding fluorescence signal: the case of dystroglycan domains. *Biophys. Chem. 107*, 197−211.
(34) Lakowicz, J. R. (2006) *Principles of fluorescence spectroscopy*, 3rd ed., Springer, New York.
(35) Krem, M. M., and Di Cera, E. (2002) Dissecting substrate recognition by thrombin using the inactive mutant S195A. *Biophys. Chem. 100*, 315−323.
(36) De Filippis, V., Frasson, R., and Fontana, A. (2006) 3-Nitrotyrosine as a spectroscopic probe for investigating protein protein interactions. *Protein Sci. 15*, 976−986.
(37) Delaglio, F., Grzesiek, S., Vuister, G. W., Zhu, G., Pfeifer, J., and Bax, A. (1995) NMRPipe: a multidimensional spectral processing system based on UNIX pipes. *J. Biomol. NMR 6*, 277−293.
(38) Collaborative Computational Project, Number 4 (1994) The CCP4 suite: programs for protein crystallography. *Acta Crystallogr., Sect. D: Biol. Crystallogr. 50*, 760−763.
(39) Emsley, P., and Cowtan, K. (2004) Coot: model-building tools for molecular graphics. *Acta Crystallogr., Sect. D: Biol. Crystallogr. 60*, 2126−2132.
(40) Joosten, R. P., Joosten, K., Cohen, S. X., Vriend, G., and Perrakis, A. (2011) Automatic rebuilding and optimization of crystallographic structures in the Protein Data Bank. *Bioinformatics 27*, 3392−3398.
(41) Morris, A. L., MacArthur, M. W., Hutchinson, E. G., and Thornton, J. M. (1992) Stereochemical quality of protein structure coordinates. *Proteins: Struct., Funct., Genet. 12*, 345−364.
(42) Bah, A., Carrell, C. J., Chen, Z., Gandhi, P. S., and Di Cera, E. (2009) Stabilization of the E* form turns thrombin into an anticoagulant. *J. Biol. Chem. 284*, 20034−20040.
(43) Pozzi, N., Chen, R., Chen, Z., Bah, A., and Di Cera, E. (2011) Rigidification of the autolysis loop enhances Na(+) binding to thrombin. *Biophys. Chem. 159*, 6−13.
(44) De Filippis, V., De Dea, E., Lucatello, F., and Frasson, R. (2005) Effect of Na+ binding on the conformation, stability and molecular recognition properties of thrombin. *Biochem. J. 390*, 485−492.
(45) Shaw, K. L., Scholtz, J. M., Pace, C. N., and Grimsley, G. R. (2009) Determining the conformational stability of a protein using urea denaturation curves. *Methods Mol. Biol. 490*, 41−55.
(46) Wells, C. M., and Di Cera, E. (1992) Thrombin is a Na(+)-activated enzyme. *Biochemistry 31*, 11721−11730.
(47) Di Cera, E., Guinto, E. R., Vindigni, A., Dang, Q. D., Ayala, Y. M., Wuyi, M., and Tulinsky, A. (1995) The Na+ binding site of thrombin. *J. Biol. Chem. 270*, 22089−22092.
(48) Bah, A., Garvey, L. C., Ge, J., and Di Cera, E. (2006) Rapid kinetics of Na+ binding to thrombin. *J. Biol. Chem. 281*, 40049−40056.
(49) Vindigni, A., De Filippis, V., Zanotti, G., Visco, C., Orsini, G., and Fontana, A. (1994) Probing the structure of hirudin from Hirudinaria manillensis by limited proteolysis. Isolation, characterization and thrombin-inhibitory properties of N-terminal fragments. *Eur. J. Biochem. 226*, 323−333.
(50) Vindigni, A., White, C. E., Komives, E. A., and Di Cera, E. (1997) Energetics of thrombin-thrombomodulin interaction. *Biochemistry 36*, 6674−6681.
(51) Stone, S. R., and Hofsteenge, J. (1986) Kinetics of the inhibition of thrombin by hirudin. *Biochemistry 25*, 4622−4628.
(52) Arosio, D., Ayala, Y. M., and Di Cera, E. (2000) Mutation of W215 compromises thrombin cleavage of fibrinogen, but not of PAR-1 or protein C. *Biochemistry 39*, 8095−8101.
(53) Di Cera, E., Dang, Q. D., Ayala, Y., and Vindigni, A. (1995) Linkage at steady state: allosteric transitions of thrombin. *Methods Enzymol. 259*, 127−144.
(54) Wang, D., Bode, W., and Huber, R. (1985) Bovine chymotrypsinogen A X-ray crystal structure analysis and refinement of a new crystal form at 1.8 A resolution. *J. Mol. Biol. 185*, 595−624.
(55) Niu, W., Chen, Z., Bush-Pelc, L. A., Bah, A., Gandhi, P. S., and Di Cera, E. (2009) Mutant N143P reveals how Na+ activates thrombin. *J. Biol. Chem. 284*, 36175−36185.
(56) Carter, W. J., Myles, T., Gibbs, C. S., Leung, L. L., and Huntington, J. A. (2004) Crystal structure of anticoagulant thrombin variant E217K provides insights into thrombin allostery. *J. Biol. Chem. 279*, 26387−26394.
(57) Gandhi, P. S., Chen, Z., Mathews, F. S., and Di Cera, E. (2008) Structural identification of the pathway of long-range communication in an allosteric enzyme. *Proc. Natl. Acad. Sci. U. S. A. 105*, 1832−1837.
(58) Jackman, M. P., Parry, M. A., Hofsteenge, J., and Stone, S. R. (1992) Intrinsic fluorescence changes and rapid kinetics of the reaction of thrombin with hirudin. *J. Biol. Chem. 267*, 15375−15383.

DOI: 10.1021/acs.biochem.6b00385
Biochemistry 2016, 55, 3984−3994